MATERIALE PLASTICE
https://revmaterialeplastice.ro
https://doi.org/10.37358/Mat.Plast.1964

Physical Properties of Biodegradable Poly(L-lactide) Induced by *N, N'*-bis(Benzoyl) 1, 3-Cyclohexanedicarboxylic Acid Dihydrazide as Crystallinity Additive

LI-SHA ZHAO, TING DENG, JUN QIAO, YAN-HUA CAI*
Chongqing Key Laboratory of Environmental Materials & Remediation Technologies, College of Chemistry and Environmental Engineering, Chongqing University of Arts and Sciences, Chongqing-402160, P.R. China

Abstract. *This work is aimed at synthesizing an organic compound N, N'-bis(benzoyl) 1,3-cyclohexane-dicarboxylic acid dihydrazide (CABH) to focus on its effect on the non-isothermal crystallization of poly(L-lactide) (PLLA), meanwhile the melting behavior, thermal decomposition process and optical property of PLLA/CABH samples in different CABH concentrations were also investigated. It was found that CABH acted as efficient heterogeneous nucleating agent for inducing PLLA's crystallization through comparative analysis of melt-crystallization process of the virgin PLLA with PLLA/CABH samples, and a high amount of CABH played a much more significant role in promoting PLLA's crystallization. Additionally, the melt-crystallization processes also showed that both the cooling rate and the final melting temperature affected the crystallization behavior of PLLA, an increase of cooling rate could weaken the crystallization ability of PLLA/CABH samples, and the final melting temperature of 180°C made PLLA/CABH exhibit the best crystallization ability. For the cold-crystallization process, the cold-crystallization peak became flatter and shifted toward the lower temperature with increasing of CABH concentration, but an increase of heating rate could prevent the cold-crystallization peak from moving to low temperature because of the thermal inertia. The melting behaviors of PLLA/CABH depended on the previous crystallization and heating rate in heating, and the difference in melting behavior of PLLA/CABH samples effectively reflected the nucleation role of CABH, as well as the double melting peaks behavior of PLLA/CABH was thought to due to the melting-recrystallization. The introduction of CABH led to a drop in light transmittance, moreover, this negative effect were more obvious with an increase of CABH loading. In contrast, the fluidity of PLLA was significantly enhanced due to the existence of CABH.*

Keywords: *poly(L-lactide), 1,3-cyclohexanedicarboxylic acid, organic nucleating agent, non-isothermal crystallization, melting behavior*

1.Introduction

The large-scale usage of the non-degradable polymeric products has led to a serious solid waste pollution, and this deterioration is getting worse in the world. Therefore, it is very urgent to develop novel sustainable materials to replace petroleum-based and non-degradable polymeric products according to the human interest, which is one of the inevitable results of promoting social sustainable development. Poly(L-lactide) (PLLA), made from renewable resources [1], has been globally considered as the most promising bio-based and degradable linear aliphatic thermoplastic polyester due to its excellent biocompatibility, safety, biodegradability [2] and mechanical properties [3], easy processing [4], and green environmental protection during the manufacture [4], etc. And these advantages have endowed PLLA with tremendous market potential in packaging fields [5-7], biomedical fields [8-11], agricultural fields [12-14], and so on. For example, the special stereocomplex networks and polyethylene glycol were introduced into PLLA to overcome its poor viscoelastic behavior, low melt strength and insufficient gas barrier properties, as well as the brittleness, the relevant results showed that, in comparison to the virgin PLLA, the elongation at break of the modified PLLA with good light transmittance increased more than 18 times, the O_2 permeability coefficient decreased by 61%, meantime, exhibiting the great potential in disposable packaging and agricultural films [15].

email: caiyh651@aliyun.com

However, the rigidity of PLLA molecular chains leads to a very slow crystallization rate comparing with the typical general plastics such as polypropylene and polyethylene [4], and this slow crystallization rate, as one of the most pressing technical challenges of PLLA [16], can bring about a low crystallinity and poor heat resistance to restrict the large-scale usage of PLLA products. For this, increasing the crystallization rate of PLLA is beneficial for adapting for applications in various fields. To date, four main methods have been employed to accelerate the crystallization of PLLA, they are adding nucleating agent or plasticizer, minimizing the amount of D-lactide isomer and adjusting the molding conditions. Compared to the other three methods, adding nucleating agent can effectively avoid the shortcomings of other methods including easy overflow, a limited crystallization accelerating effect, difficulty in obtaining the low D-lactide content and an increase of the higher energy consumption [4, 17], and induces the crystallization at high temperature region or fast cooling rate through reducing the surface free energy barrier toward nucleation [18], which has been considered as an efficient and the easiest way in industry to tailor the crystallization of PLLA [17, 19]. The natural minerals, including talc [20, 21], montmorillonite [22, 23], halloysite [24, 25], were focused to act as the nucleating agent of PLLA because of their low cost, especially the introduction of talc could make the half time of overall PLLA crystallization reduce by an order of magnitude [26], exhibiting very advanced nucleation ability. Additionally, many other inorganic or organic compounds were also successively developed to be as the nucleating agents for PLLA's crystallization, apart from the natural minerals, the typical inorganic nucleating agents include calcium carbonate [27, 28], zinc phenylphosphonate [29, 30], MgO [31, 32], and so on. The organic nucleating agents for PLLA were firstly selected from the commercial organic nucleating agents for other semi-crystalline polymers like EBS [33] and phthalimide [34]. And then according to the continuous exploration of PLLA crystallization process, some new organic nucleating agents with specific functional groups or space structures had been synthesized to evaluate their effects on the PLLA's crystallization, and the typical synthesized organic nucleating agents include benzoyl hydrazine derivatives [35, 36], oxalamide derivatives [37, 38], piperonylic acid derivatives [39, 40], 1H-benzotriazole derivatives [41, 42] and urea derivatives [43]. Moreover, the more attentions have also been focused on the organic nucleating agents because of their better compatibility with PLLA [44]. Given that, the nucleation effect of organic compounds is still far from the acceptable for industrial requirements, the key reason depends on the undefined nucleation mechanism, whereas the nucleation mechanism must establish the structure-property relationships of molecular structure of a larger amount of organic nucleating agents with PLLA crystallization ability. Unfortunately, the quantity and category of organic nucleating agents are insufficiently comparing with the inorganic nucleating agents. For this, the current work is the first to synthesis an organic compound *N, N'*-bis(benzoyl) 1,3-cyclohexane-dicarboxylic acid dihydrazide (designated here as CABH) as a crystallinity additive to evaluate its influence on the non-isothermal crystallization behavior of PLLA in detailed, and the melting behavior, thermal decomposition in air and optical property of CABH-nucleated PLLA were further investigated by differential scanning calorimeter (DSC), transmittance instrument and melt index meter. This work is meaningful to rich the category and increase the number of organic nucleating agents, it is also helpful to further explore the structure-activity relationship and nucleation mechanism.

2. Materials and methods

Reagents and materials

All reagents used to synthesis CABH were analytically pure, and these reagents, including 1,3-cyclo-hexanedicarboxylic acid, thionyl chloride, benzoic hydrazide, pyridine and *N*,*N*-dimethyl-formamide (DMF), were supplied by Chongqing Huanwei Chemical Company of China; in addition, all reagents were directly used as received without purification in this study. The commercial grade 4032D PLLA was produced by Nature Works LLC of USA.

Synthesis of CABH

As seen in Figure 1, the synthesis of CABH was completed *via* the acylation of 1,3-cyclohexane-dicarboxylic acid as the first step reaction and the amination of cyclohexyl-1, 3-dicarboxylchloride and benzoic hydrazide as the second step reaction. First, the 10 g 1, 3-cyclohexanedicarboxylic acid was added into the mixed solution of 80 mL thionyl chloride as the reactant and solvent and the 2 mL DMF as catalyst. The aforementioned mixture was slowly heated up to 80°C with stirring to dissolve the solid-state 1, 3-cyclohexanedicarboxylic acid, and formed the reflux through the water cooling, as well as held at 80°C for 36 h. After that, the vacuum distillation of the mixed solution were performed to obtain the cyclohexyl-1, 3-dicarboxylchloride. Second, the 0.01 mol benzoic hydrazide and 2 mL pyridine was dissolved into the 60 mL DMF as solvent to form the mixed solution, and the 0.005 mol cyclohexyl-1, 3-dicarboxylchloride was rapidly added into the aforementioned mixed solution to stir at room temperature for 1 h, heated up to 70°C for 3 h with stirring. Finally, the mixed solution was poured into 300 ml water to form the suspension, and the suspension was filtrated and washed for 3 times. The resulting product was thoroughly dried in vacuum. Fourier Transform Infrared Spectrometer (FT-IR) υ: 3373.7, 1679.0, 1636.9, 1598.0, 1576.6, 1527.0, 1500.6, 1477.4, 1446.6, 1384.8, 1346.9, 1328.7, 1287.6, 1256.6, 1225.3, 1180.6, 1147.6, 1123.8, 1096.0, 1076.2, 1025.9, 903.1, 873.9, 802.6, 692.8 cm^{-1}; ^1H Nuclear Magnetic Resonance (^1H NMR) δ: ppm; 10.32 (s, 1H, NH), 9.88 (s, 1H, NH), 7.48~7.88 (m, 5H, Ph), 2.37 (s, 1H, CH), 1.80~1.91 (m, 2H, CH2) 1.55~1.64 (m, 1H, CH), 1.35~1.39 (t, 1H, CH).

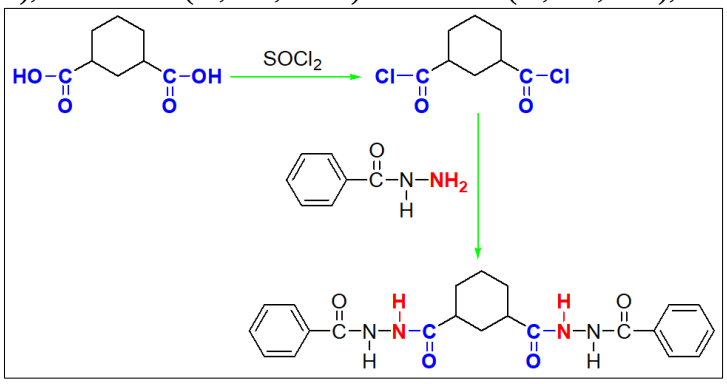

Figure 1. Synthetic route of CABH

Preparation of PLLA/CABH samples

To avoid the effect of residual water during the melting blend, the mixture of PLLA and CABH must be dried for 24 h at 45°C to remove the residual water. The mass ratio of PLLA and CABH were 100/0, 99.5/0.5, 99/1, 98/2 and 97/3, respectively; and the relevant samples were named as the virgin PLLA, PLLA/0.5%CABH, PLLA/1%CABH, PLLA/2%CABH and PLLA/3%CABH. The detailed melting blend was performed on a torque rheometer with blending temperature of 190°C, and the blending time was set at the rotation speed of 32 rpm for 7 min and the rotation speed of 64 rpm for 7 min. After the melting blend, the mixture was pressed into thin sheets with a thickness of 0.4 mm *via* hot-pressing at 180°C and cool-pressing at room temperature under 20 MPa.

Testing and characterizations

The characterization of CABH molecular structure was perfomed on a Nicolet iS50 FT-IR and Bruker 400MHz ^1H NMR. Before FT-IR characterization, the testing CABH sample was prepared using KBr pellet, and the wavenumber was set from 4000 cm^{-1} to 400 cm^{-1}, the obtained infrared spectrum was analyzed according to the characteristic absorption of the related groups. The CABH was dissolved in methyl sulfoxide to perform the ^1H NMR characterization, and the chemical shift and integral area were analyzed to further determine the CABH molecular structure. The non-isothermal crystallization behavior of the relevant samples were recorded by TA instrument Q2000 DSC with 50 mL/min nitrogen. Before DSC testing, on one hand, the temperature and heat flow were calibrated using an indium standard; on the other hand, all samples were heated to 190°C for 3 min for eliminating thermal history

to ensure the test at the same level. For light transmittance, the average value of the 5 times light transmittance measurements was used as the light transmittance of a given sample. The melt index instrument was used to test fluidity, and the testing temperature was set at 180ºC.

3.Results and discussions

Non-isothermal crystallization

Figure 2 illustrates the DSC thermograms of the PLLA with and without CABH from the melt of 190°C at a cooling rate of 1°C/min. Based on these DSC curves, it is found that the virgin PLLA has almost no melt-crystallization peak upon cooling at 1°C/min, showing a poor crystallization ability of the virgin PLLA. In contrast with the virgin PLLA, the crystallization of PLLA was significantly enhanced in the presence of CABH, because all PLLA/CABH samples have obvious and sharp melt-crystallization peak in DSC curves. Clearly, this difference depends on the CABH, CABH as a heterogeneous nucleus can provide the high nucleation density in PLLA matrix to promote the crystallization. Additionally, Figure 2 also shows the effect of CABH concentration on the melt-crystallization of PLLA, with increasing of CABH centration from 0.5 wt% to 3 wt%, the melt-crystallization peak becomes sharper, meaning that the crystallization rate is continuously accelerated by a higher CABH concentration. Meanwhile, a higher CABH concentration makes the melt-crystallization peak shift toward the higher temperature, which further confirms the nucleation effect of CABH for PLLA's crystallization, because the role of nucleating agent is to induce the crystallization to occur at a higher temperature. The relevant crystallization parameters of the onset crystallization temperature (T_{oc}), melt-crystallization peak temperature (T_{cc}) and melt-crystallization enthalpy (ΔH_c) were obtained from the DSC curves. Compared to the PLLA/0.5%CABH sample, the T_{oc}, T_{cc} and ΔH_c of PLLA/3%CABH sample increase from 120.0°C, 112.6°C and 42.3 J/g to 138.1°C, 134.5°C and 49.8 J/g, respectively, and the difference between T_{oc} and T_{cc} (ΔT_c) decreases from 7.4°C to 3.6°C, showing a faster crystallization rate.

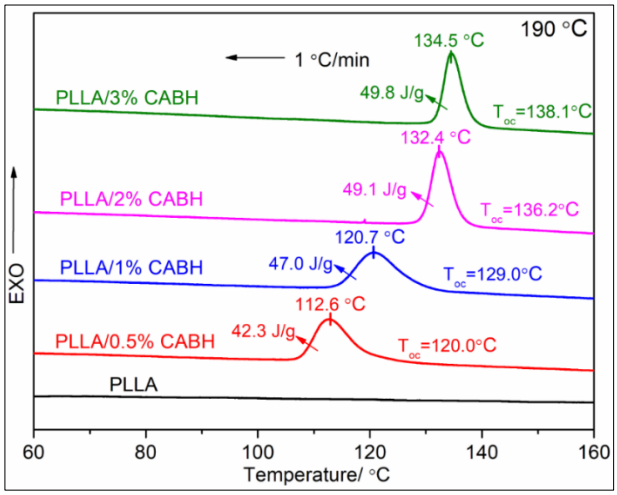

Figure 2. DSC curves of the virgin PLLA and PLLA/CABH samples from the melt of 190°C at a cooling rate of 1°C/min

To meet the requirement of actual production, it is necessary to investigate the crystallization behavior upon cooling at a faster rate. Figure 3 is the DSC thermograms of PLLA/CABH from the melt of 190°C at different cooling rates (10°C/min and 20°C/min). It is observed from Figure 3 that the melt-crystallization peak becomes flatter with increasing of cooling rate from 10°C/min to 20°C/min, and when the cooling rate is 20°C/min, excepting the PLLA/3%CABH sample, the melt-crystallization peaks of other PLLA/CABH samples cannot almost be detected in DSC curves, indicating that the cooling rate is an important factor for the melt-crystallization behavior of PLLA in cooling. It should be also noted that PLLA containing a high CABH concentration has an inhibition for the decrease of PLLA/CABH crystallization ability, because the melt-crystallization peak of PLLA with a low CABH concentration is easier to be weakened with increasing of cooling rate comparing with the PLLA with a high CABH

concentration, indicating that a high CABH concentration exhibits the better crystallization accelerating effect for PLLA's crystallization, which is proved by the result of melt-crystallization from the melt of 190°C at a cooling rate of 1°C/min.

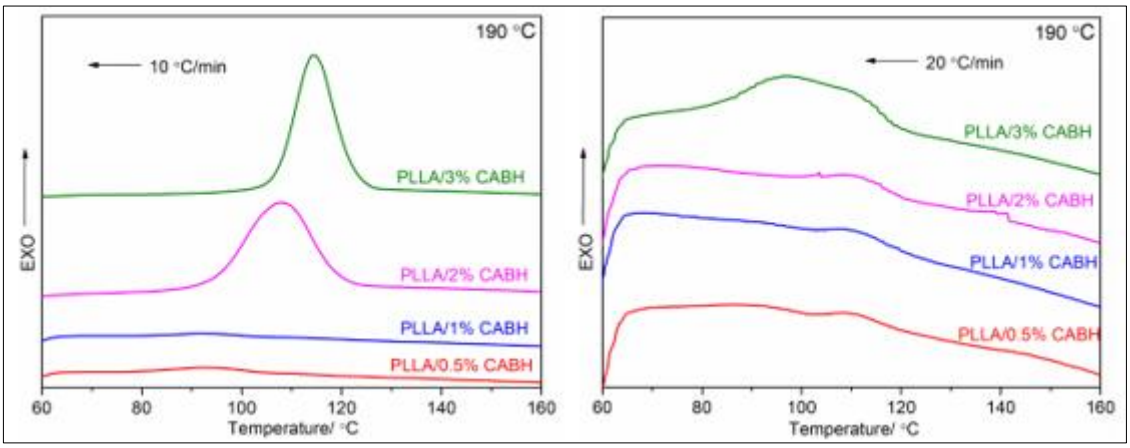

Figure 3. DSC curves of PLLA/CABH samples from the melt of 190°C at various cooling rates

For actual production, exploring the optimum processing temperature combination is meaningful due to the distinct effect of the final melting temperature (T_f) on the crystallization behavior as reported [42, 45, 46]. For the organic additive, the T_f can directly affect the solubility of CABH in PLLA matrix and influences the amount of undissolved BACH. That is, a higher T_f can increase the solubility of CABH, which promotes more CABH to be dissolved in PLLA matrix and enhances the compatibility of PLLA with CABH; but a decrease of undissolved CABH concentration must reduce the nucleation density of PLLA resin. As a result, this relationship of the aforementioned mutual restriction will make the crystallization process become uncertain. Figure 4 displays the melt-crystallization behaviors of four PLLA/CABH samples from the different T_f at a heating rate of 1°C/min, and the relevant crystallization parameters were listed in Table 1. As shown in Figure 4, When the T_f is 170°C, all PLLA/CABH samples exhibit very wide melt-crystallization peaks in DSC curves, and the minimum ΔT_c is up to 7.3°C, which is very close to the maximum ΔT_c of 7.4°C when the T_f is 190°C, implying that the T_f of 170°C weakens the crystallization ability of PLLA/CABH, the probable reason is that the relative low T_f and more undissolved CABH remarkably restricts the efficient migration of PLLA molecular chain in cooling, although the low T_f is conducive to nucleation. As a result, it takes more time to complete the crystallization at a lower temperature. However, when the T_f is 180°C, the other PLLA/CABH samples exhibit the higher T_{oc}, T_{cc} and the larger ΔH_c except the PLLA/1%CABH sample, indicating that the 180°C in general is the optimum T_f compared with the T_f of 170°C and 190°C.

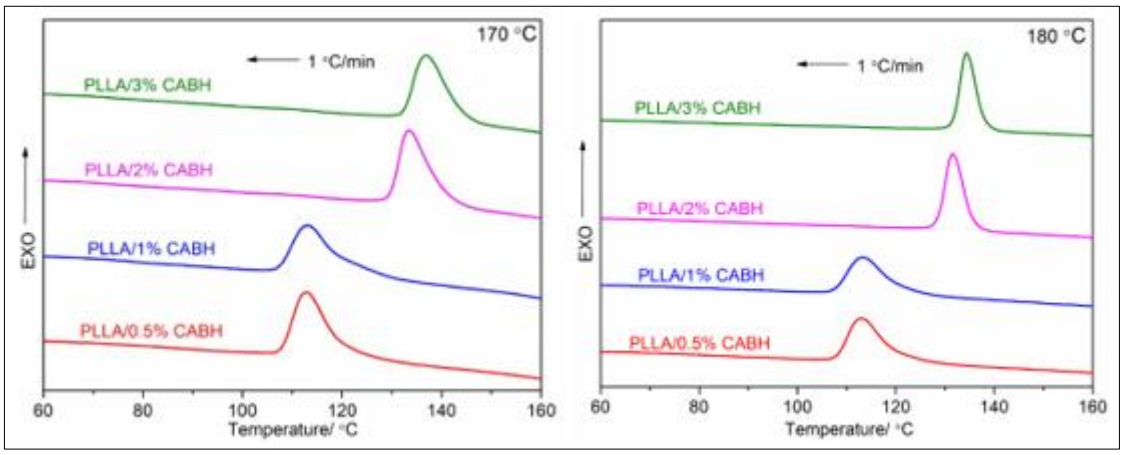

Figure 4. Melt-crystallization DSC curves of PLLA/CABH from different T_f

Table 1. Melt-crystallization parameters of PLLA/CABH from the different T_f

T_f / °C	Sample	T_{oc} / °C	T_{mc} / °C	ΔH_c / J/g
170	PLLA/0.5%CABH	120.2	112.9	44.3
	PLLA/1%CABH	121.3	113.2	42.8
	PLLA/2%CABH	141.0	133.5	54.1
	PLLA/3%CABH	144.4	137.0	53.6
180	PLLA/0.5%CABH	120.8	113.0	46.4
	PLLA/1%CABH	121.5	113.4	45.5
	PLLA/2%CABH	135.6	131.6	51.9
	PLLA/3%CABH	137.9	134.4	49.9

The cold-crystallization behavior of PLLA/CABH was also further studied by DSC. Figure 5 is the cold-crystallization DSC curves of PLLA/CABH samples from 40°C to 180°C at the heating rate of 1°C/min and 5°C/min. It is clear that there are obvious cold-crystallization peaks and the single melting peak in all DSC curves. When the heating rate is 1°C/min, the cold-crystallization peak shifts toward the lower temperature side with an increase of CABH concentration, similar effect of other nucleating agents on the cold-crystallization temperature of PLLA could be found in literature [47]. In contrast, the cold-crystallization peak moves toward the higher temperature side overall upon the heating at 5°C/min, evidently, this effect depends on the heating rate. That is to say, at a slow heating rate, a higher CABH loading can induce the crystallization to occur at a lower temperature due to the larger nucleation density, but a larger amount of CABH must exhibit the greater hindering the segmental mobility of PLLA, resulting in that the weaker and wider cold-crystallization peak appears at a lower temperature. However, when the heating rate is increased to 5°C/min, the thermal inertia promotes the cold-crystallization peak to shift to the higher temperature side. Additionally, upon the heating at 1°C/min, the melting peak temperatures of all PLLA/CABH samples are higher as compared with that these temperatures from the melting peak at the heating rate of 5°C/min, the reason is that the crystals are more perfect at the heating rate of 1°C/min, which is proved by the sharper cold-crystallization peaks.

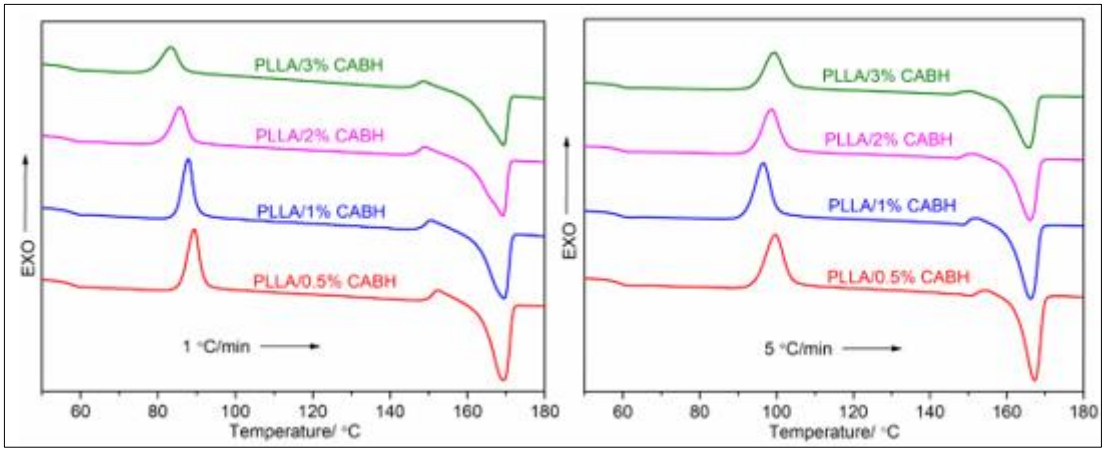

Figure 5. Cold-crystallization DSC curves of PLLA/CABH at various heating rates

Melting process

The melting processes of PLLA/CABH samples after different crystallization conditions were also recorded by DSC. Figure 6 is the melting behavior of PLLA/CABH samples at the heating rate of 1 °C/min or 5°C/min after cooling at 1°C/min. It is very obvious that there exist the double melting peaks in DSC curves, furthermore, the peak area ratio of low-temperature side melting peak and high-temperature side melting peak upon heating at 5°C/min is larger than that upon heating at 1°C/min, but the melting temperature of high-temperature side peak is lower, because the recrystallization phenomenon will occur in heating according to the melting-recrystallization mechanism of double melting peaks [48]. On one hand, a high heating rate can form the relatively imperfect crystals, resulting in that the high-temperature side melting peak appears at the lower temperature; however; on the other hand, a high heating rate can also make the peak shift to higher temperature because of the thermal inertia. Under this circumstance, the effect of the relatively imperfect crystals is greater.

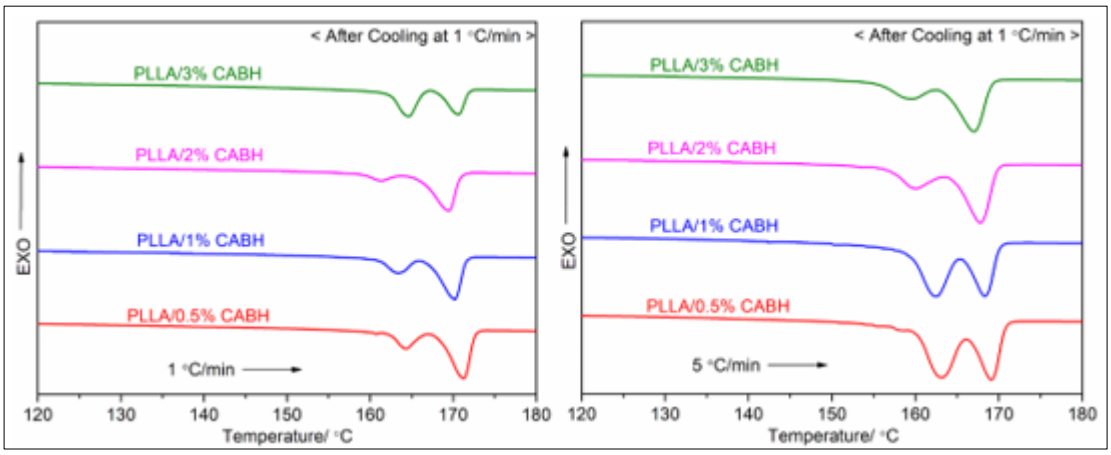

Figure 6. Melting processes of PLLA/CABH samples at various heating rates after melt-crystallization upon cooling at 1°C/min

Figure 7 is the melting DSC curves of PLLA/CABH samples at the heating rate of 10°C/min after isothermal crystallization at various crystallization temperatures for 180 min. For the melting behavior after isothermal crystallization, the melting behavior was significantly affected by the crystallization temperature as shown in Figure 8. When the crystallization temperature is 115°C, all PLLA/CABH samples have the double melting peaks in DSC curves, whereas the single melting peak appears in heating after isothermal crystallization at 135°C, showing that the low crystallization temperature cannot cause the crystallization be thoroughly completed, even if the crystallization time is long enough, the root reason for this result is the effect of mobility of PLLA molecular chain in low-temperature region. In contrast, a high crystallization temperature ensures the excellent mobility of PLLA molecular chain, meantime, the existence of CABH can provide the heterogeneous nucleus for crystallization, as well as the crystallization time is so long enough that the crystallization can be completed, as a result, DSC curves in heating has only a single melting peak. However, the melting peak after crystallization at 135°C shifts toward the low-temperature side with increasing of CABH concentration, resulting from the hindrance effect of CABH concentration on the migration of PLLA molecular chain and crystal growth.

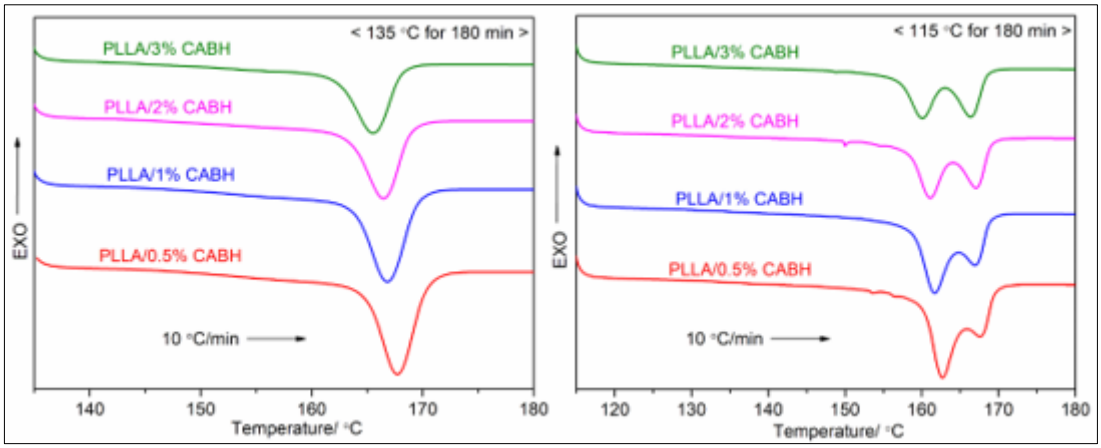

Figure 7. Melting curves of PLLA/CABH samples at the heating rate of 10°C/min after isothermal crystallization at 115°C and 135°C

Optical property and fluidity

The light transmittances of the virgin PLLA and CABH-nucleated PLLA was compared in Figure 8. At the range of CABH concentration, the effect of CABH on the light transmittance of PLLA can be classified into two types. When the CABH concentration is lower than 0.5 wt%, the light transmittance shows a very small decline; when the CABH concentration is further increased to 1 wt%, the light transmittance is decreased from 78.2% to 44.8% compared to the virgin PLLA; and when the CABH concentration is higher than 1 wt%, the light transmittance exhibits a drastic decline, even the light transmittance of PLLA/3%CABH is only 2.6%. This effect might be because of two reasons, the main reason is that the white CABH can decrease the light transmittance of PLLA, and the higher the CABH concentration is, the worse the light transmittance drops; another probable reason is that CABH can promote the crystallization of PLLA more or less in the process, leading to a higher crystallinity, and an increase of crystallinity must decrease the light transmittance of PLLA.

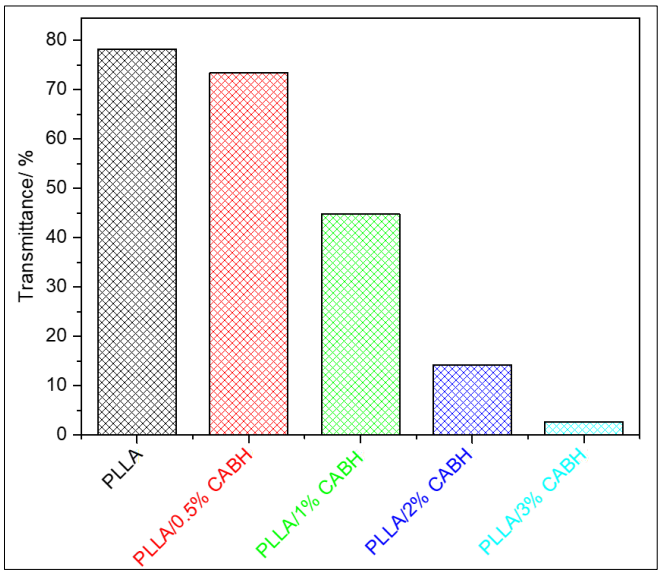

Figure 8. Light transmittances of the virgin PLLA and PLLA/CABH samples

The melt flow rate (MFR) is measured to determine polymer's fluidity, and the larger the MFR value is, the better the fluidity is. Figure 9 is MFR of PLLA with CABH and without CABH. It is observed that the existence of CABH significantly enhances PLLA's fluidity, and the MFR value of any PLLA/CABH is more than nine times than that of the virgin PLLA. The aforementioned result indicates

that the CABH may weaken the intermolecular interaction of PLLA molecular chains and promote mobility of PLLA molecular chain. However, the MFR cannot continuously increase as CABH concentration increased, specifically, when the CABH concentration is 0.5 wt% to 2 wt%, the MFR can increases from 15.4 g/10min to the largest value of 22.4 g/10min. When the CABH concentration is further increased to 3 wt%, the MFR begins to fall, the reason may be that an excessive dose of CABH exhibits a greater inhibition for mobility of PLLA molecular chain comparing with the positive effect of CABH for weakening the intermolecular interaction of PLLA molecular chains.

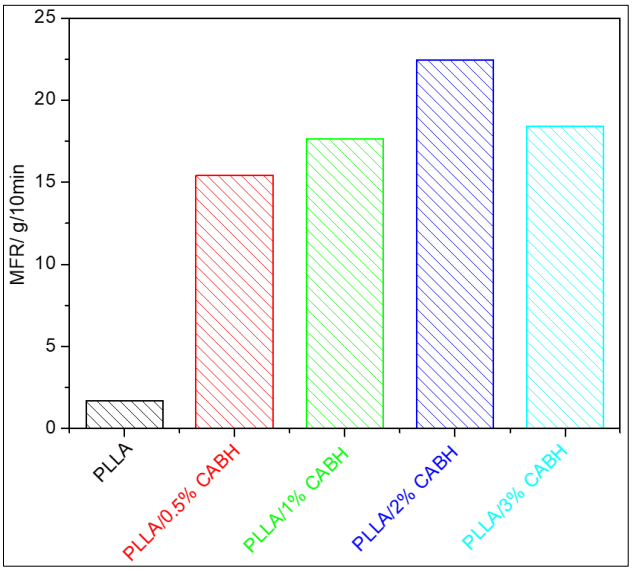

Figure 9. MFR of PLLA and PLLA/CABH

4.Conclusions

1, 3-cyclohexanedicarboxylic acid derivative CABH was synthesized to be as the organic nucleating agent for PLLA's crystallization, and the CABH-nucleated PLLA were fabricated using a torque rheometer. The melt-crystallization processes showed that the CABH acted as effective promoting agent for the crystallization of PLLA in cooling. With increasing of CABH concentration, PLLA/CABH sample exhibited the greater crystallization ability in cooling at 1°C/min, and the T_{oc}, T_{cc} and ΔH_c of PLLA/3%CABH sample were up to the maximum value of 138.1°C, 134.5°C and 49.8 J/g, respectively. However, an increase of cooling rate seriously weakened the crystallization ability, when the cooling rate was 20°C/min, the melt-crystallization peaks of the most of PLLA/CABH samples could almost not be observed. The effect of the T_f on the melt-crystallization process of PLLA indicated that the T_f of 180°C was more conducive to crystallization of PLLA/CABH comparing with the other T_f in this study. Upon heating at 1°C/min, the CABH had an inhibition for the cold crystallization process of PLLA, because the cold-crystallization peak became flatter and shifted toward the lower temperature with increasing of CABH concentration, however, an increase of heating rate could promoted the cold-crystallization to be a shift toward the high-temperature side. The melting behavior of PLLA/CABH after melt-crystallization at the cooling rate of 1°C/min showed that there existed the double melting peaks in DSC curves resulting from the melting-recrystallization, and the heating rate could cause the peak area ratio between low-temperature side melting peak and high-temperature side melting peak to become larger. Additionally, the crystallization temperature also significantly affected the melting behavior, and PLLA/CABH had only a single melting peak after isothermal crystallization at a relative high crystallization temperature, in contrast with the double melting peak after isothermal crystallization at a low crystallization temperature. The light transmittance was decreased because of the synergistic effects of white CABH itself and an increase of crystallinity. However, the introduction of CABH could

make fluidity of PLLA increase more than nine times comparing with the virgin PLLA, primarily resulting from the weakening of intermolecular interaction.

Acknowledgements. This work was supported by National Natural Science Foundation of China (project number 51403027), Foundation of Chongqing Municipal Science and Technology Commission (cstc2019jcyj-msxmX0876), as well as Scientific and Technological Research Program of Chongqing Municipal Education Commission (project number KJQN201801319).

References

1. SOMSUNAN R, MAINOIY N., Isothermal and non-isothermal crystallization kinetics of PLA/PBS blends with talc as nucleating agent [J], Journal of Thermal Analysis and Calorimetry, 2020, 139(3): 1941-1948
2.YU MH, ZHENG YJ, TIAN JZ., Study on the biodegradability of modified starch/polylactic acid (PLA) composite materials [J], RSC Advances, 2020, 10(44): 26298-26307
3.JI N, HU G, LI JB, REN J., Influence of poly(lactide) stereocomplexes as nucleating agents on the crystallization behavior of poly(lactide)s [J], RSC Advances, 2019, 9(11): 6221-6227
4.CHEN P, ZHOU HF, LIU W, ZHANG M, DU ZJ, WANG XD., The synergistic effect of zinc oxide and phenylphosphonic acid zinc salt on the crystallization behavior of poly (lactic acid) [J], Polymer Degradation and Stability, 2015, 122: 25-35
5.NAZRIN A, SAPUAN SM, ZUHRI MYM, ILYAS RA, SYAFIQ R, SHERWANI SFK., Nanocellulose reinforced thermoplastic starch (TPS), polylactic acid (PLA), and polybutylene succinate (PBS) for food packaging applications [J], Frontiers in Chemistry, 2020, 8: 213
6.PIETROSANTO A, SCARFATO P, DI MAIO L, NOBILE MR, INCARNATO L., Evaluation of the suitability of poly(lactide)/poly(butylene-adipate-co-terephthalate) blown films for chilled and frozen food packaging applications [J], Polymers, 2020, 12(4): 804
7. YUN XY, LI XF, DONG T., Preparation and Characterization of Poly(L-lactic acid) Coating Film for Strawberry Packaging [J], Science of Advanced Materials, 2019, 11(10): 1488-1499
8. CHIESA E, DORATI R, PISANI S, BRUNI G, RIZZI LG, CONTI B, MODENA T, GENTA I. Graphene Nanoplatelets for the Development of Reinforced PLA-PCL Electrospun Fibers as the Next-Generation of Biomedical Mats [J], Polymers, 2020, 12(6): 1390
9. CESUR S, OKTAR FN, EKREN N, KILIC O, ALKAYA DB, SEYHAN SA, EGE ZR, LIN CC, ERDEM S, ERDEMIR G, GUNDUZ O., Preparation and characterization of electrospun polylactic acid/sodium alginate/orange oyster shell composite nanofiber for biomedical application [J], Journal of the Australian Ceramic Society, 2020, 56(2): 533-543
10.SINGHVI MS, ZINJARDE SS, GOKHALE DV., Polylactic acid: synthesis and biomedical applications [J], Journal of Applied Microbiology, 2019, 127(6): 1612-1626
11.ELMOWAFY ENAS M, TIBONI MATTIA, SOLIMAN MAHMOUD E., Biocompatibility, biodegradation and biomedical applications of poly(lactic acid)/poly(lactic‐co‐glycolic acid) micro and nanoparticles [J], Journal of Pharmaceutical Investigation, 2019, 49(4): 347-380
12. KHAN H, KAUR S, BALDWIN TC, RADECKA I, JIANG GZ, BRETZ I, DUALE K, ADAMUS G, KOWALCZUK M., Effective control against broadleaf weed species provided by biodegradable PBAT/PLA mulch film embedded with the herbicide 2-methyl-4-chlorophenoxyacetic acid (MCPA) [J], ACS Sustainable Chemistry & Engineering, 2020, 8(13): 5360-5370
13. FRANCA DC, ALMEIDA TG, ABELS G, CANEDO EL, CARVALHO LH, WELLEN RMR, HAAG K, KOSCHEK K., Tailoring PBAT/PLA/Babassu films for suitability of agriculture mulch application [J], Journal of Natural Fibers, 2019, 16(7): 933-943
14. MOSNACKOVA K, SISKOVA A, JANIGOVA I, KOLLAR J, SLOSAR M, CHMELA S, ALEXY P, CHODAK I, BOCKAJ J, MOSNACEK J., Ageing of plasticized poly(lactic acid)/poly(beta-hydroxybutyrate) blend films under artificial UV irradiation and under real agricultural conditions during their application as mulches [J], Chemical Papers, 2016, 70(9): 1268-1278

15. JIANG YP, YAN C, WANG K, SHI DW, LIU ZY, YANG MB., Super-toughed PLA blown film with enhanced gas barrier property available for packaging and agricultural applications [J], Materials, 2019, 12(10): 1663
16. GENG ZX, ZHEN WJ, SONG ZB, WANG XF., Structure and performance of poly(lactic acid)/amide ethylenediamine tetraacetic acid disodium salt intercalation layered double hydroxides nanocomposites [J], Journal of Polymer Research, 2018, 25: 115
17. CAI YH, YAN SF, FAN YQ, YU ZY, CHEN XS, YIN JB., The nucleation effect of *N*, *N'*-bis(benzoyl) alkyl diacid dihydrazide on crystallization of biodegradable poly(L-lactic acid) [J], Iranian Polymer Journal, 2012, 21(7): 435-444
18. FENG YQ, MA PM, XU PW, WANG RY, DONG WF, CHEN MQ, JOZIASSE C., The crystallization behavior of poly(lactic acid) with different types of nucleating agents [J], International Journal of Biological Macromolecules, 2018, 106: 955-962
19. KHWANPIPAT T, SEADAN M, SUTTIRUENGWONG S., Effect of PDLA and amide compounds as mixed nucleating agents on crystallization behaviors of poly(L-lactic acid) [J], Materials, 2018, 11(7): 1139
20. LI Y, HAN CY, YU YC, XIAO LG, SHAO Y., Effect of content and particle size of talc on nonisothermal melt crystallization behavior of poly(L-lactide) [J], Journal of Thermal Analysis and Calprimetry, 2019, 135(4): 2049-2058
21. KOVALCIK A, PEREZ-CAMARGO RA, FURST C, KUCHARCZYK P, MULLER AJ., Nucleating efficiency and thermal stability of industrial non-purified lignins and ultrafine talc in poly(lactic acid) (PLA) [J], Polymer Degradation and Stability, 2017, 142: 244-254
22. CHEN WT, CHEN H, YUAN Y, PENG SX, ZHAO XP., Synergistic effects of polyethylene glycol and organic montmorillonite on the plasticization and enhancement of poly(lactic acid) [J], Journal of Applied Polymer Science, 2019, 136(21): 47576
23. LI XX, YIN JB, YU ZY, YAN SF, LU XC, WANG YJ, CAO B, CHEN XS., Isothermal crystallization behavior of poly(L-lactic acid)/organo-montmorillonite nanocomposites [J], Polymer Composites, 2009, 30(9): 1338-1344
24. GUO JH, QIAO JX, ZHANG X., Effect of an alkalized-modified halloysite on PLA crystallization, morphology, mechanical, and thermal properties of PLA/halloysite nanocomposites [J], Journal of Applied Polymer Science, 2016, 133(48): 44272
25. KAYGUSUZ I, KAYNAK C., Influences of halloysite nanotubes on crystallisation behaviour of polylactide [J], Plastics Rubber and Composites, 2015, 44(2): 41-49
26. KE TY, SUN XZ., Melting behavior and crystallization kinetics of starch and poly(lactic acid) composites [J], Journal of Applied Polymer Science, 2003, 89(5): 1203-1210
27. PHETWAROTAI W, AHT-ONG D., Nucleated polylactide blend films with nanoprecipitated calcium carbonate and talc [J], Journal of Thermal Analysis and Calorimetry, 2017, 127(3): 2367-2381
28. DE ALMEIDA JFM, DA SILVA ALN, ESCOCIO VA, DA SILVA AHMDT, DE SOUSA AMF, Nascimento CR, Bertolino LC. Rheological, mechanical and morphological behavior of polylactide/ nano-sized calcium carbonate composites[J], Polymer Bulletin, 2016, 73(12): 3531-3545
29. YANG TC, HUNG KC, WU TL, WU TM, WU JH., A comparison of annealing process and nucleating agent (zinc phenylphosphonate) on the crystallization, viscoelasticity, and creep behavior of compression-molded poly(lactic acid) blends [J], Polymer Degradation and Stability, 2015, 121: 230-237
30. PAN PP, LIANG ZC, CAO A, INOUE Y., Layered metal phosphonate reinforced poly(L-lactide) composites with a highly enhanced crystallization rate[J], ACS Applied Materials & Interfaces, 2009, 1(2): 402-411
31. WEN W, LU YT, QIN XP, LUO BH, ZHOU CR., Effect of MgO whiskers on thermal behavior and mechanical properties of injection molded poly(L-lactide) [J], Polymer Composites, 2018, 39: E1807-E1820

32. JIA JP, YANG JJ, ZHAO Y, LIANG H, CHEN MF. The crystallization behaviors and mechanical properties of poly(L-lactic acid)/magnesium oxide nanoparticle composites [J], RSC Advances, 2016, 6(50): 43855-43863
33. HARRIS AM, LEE EC. Improving mechanical performance of injection molded PLA by controlling crystallinity [J], Journal of Applied Polymer Science, 2008, 107(4): 2246-2255
34. HE DR, WANG YM, SHAO CG, ZHENG GQ, LI Q, SHEN CY. Effect of phthalimide as an efficient nucleating agent on the crystallization kinetics of poly(lactic acid) [J], Polymer Testing, 2013, 32: 1088-1093
35. ZOU GX, JIAO QW, ZHANG X, ZHAO CX, LI JC. Crystallization behavior and morphology of poly(lactic acid) with a novel nucleating agent [J], Journal of Applied Polymer Science, 2015, 132(5): 41367
36. CAI YH, YAN SF, YIN JB, FAN YQ, CHEN XS., Crystallization behavior of biodegradable poly(L-lactic acid) filled with a powerful nucleating agent: *N,N'*-bis(benzoyl) suberic acid dihydrazide [J], Journal of Applied Polymer Science, 121(3): 1408-1416
37. SHEN TF, XU YS, CAI XX, MA PM, DONG WF, CHEN MQ., Enhanced crystallization kinetics of poly(lactide) with oxalamide compounds as nucleators: effect of space length beyween the oxalamide moieties[J], RSC Advances, 2016, 6(54): 48365-48374
38. MA PM, XU YS, WANG DW, DONG WF, CHEN MQ., Rapid crystallization of poly(lactic acid) by using tailor-made oxalamide derivatives as novel soluble-type nucleating agents[J], Industrial & Engineering Chemistry Research, 2014, 53(32): 12888-12892
39. ZHAO LS, CAI YH., Insight on the effect of a piperonylic acid derivative on the crystallization process, melting behavior, thermal stability, optical and mechanical properties of poly(L-lactic acid) [J], E-Polymers, 2020, 20: 203-213
40. ZHAO LS, CAI YH., Non-isothermal crystallization, melting behavior, thermal decomposition, fluidity and mechanical properties of melt processed poly(L-lactic acid) nucleated by *N, N'*-adipic bis(piperonylic acid) dihydrazide [J], Polymer Science, Series A, 2020, 62(4): 343-353
41. CAI YH, TANG Y, ZHAO LS., Poly(L-lactic acid) with the organic nucleating agent *N, N, N*-tris(1H-benzotriazole) trimesinic acid acethydrazide: Crystallization and melting behavior [J], Journal of Applied Polymer Science, 132(32): 42402
42. CAI YH, ZHAO LS., Thermal behavior of modified poly(L-lactic acid): effect of aromatic multiamide derivative based on 1H-benzotriazole [J], E-Polymers, 2016, 16(4): 303-311
43. XU YT, WU LB. Synthesis of organic bisurea compounds and their roles as crystallization nucleating agents of poly(L-lactic acid) [J], European Polymer Journal, 2013, 49: 865-872
44. ZHENG L, ZHEN WJ. Preparation and characterization of amidated grapheme oxide and its effect on the performance of poly(lactic acid) [J], Iranian Polymer Journal, 2018, 27: 239-252
45. FAN YQ, ZHU J, YAN SF, CHEN XS, YIN JB., Nucleating effect and crystal morphology controlling based on binary phase behavior between organic nucleating agent and poly(L-lactic acid) [J], Polymer, 2015, 67: 63-71
46. KONG WL, ZHU B, SU FM, WANG Z, SHAO CG, WANG YM, LIU CT, SHEN CY., Melting temperature, concentration and cooling rate-dependent nucleating ability of a self-assembly aryl amide nucleator on poly(lactic acid) crystallization [J], Polymer, 2019, 168: 77-85
47. SUKSUT B, DEEPRASERTKUL C. Effect of nucleating agents on physical properties of poly(lactic acid) and its blend with natural rubber [J], 2011, Journal of Polymers and the Environment, 2011, 19(1): 288-296
48. YASUNIWA M, TSUBAKIHARA S, SUGIMOTO Y, NAKAFUKU C., Thermal analysis of the double-melting behavior of poly(L-lactic acid) [J], Journal of Polymer Science: Part B: Polymer Physics, 2004, 42(1): 25-32

Manuscript received: 13.03.2021